Response to reviewer's comments (RC1)
Spatiotemporal heterogeneity in the increase of ocean acidity extremes in the Northeast Pacific

Flora Desmet, Matthias Münnich, and Nicolas Gruber

October 26, 2023

General remarks

First and foremost, we thank the editor and this reviewer for their very supportive and insightful comments on our manuscript. We appreciate the valuable remarks that helped us to significantly improve the quality of this manuscript.

Many of the reviewer's comments center on two issues: (i) the comparison of the modeled subsurface fields with observations, and (ii) the role of changes in $[H^+]$ variability on the increase of OAX. In response to (i), we added an evaluation of the simulated subsurface trends in dissolved inorganic carbon using observations from a repeat transect to station "P" in the Northeast Pacific. In response to (ii), we added a discussion paragraph on the contribution of changes in $[H^+]$ variability to OAX increase together with an additional appendix figure. Based on the reviewer's comments, we also clarified the role and impact of the southern boundary of the model. In addition to the responses to the reviewer's comments, we updated a few numbers, due to our recent noticing that we had used an improper area weighting of spatial averages in our initial submission. These updates are very minor and have no implications for the key findings and messages of the manuscript.

Herein, we provide a summary of each of the reviewer's comments (RC1) in black, followed by our point by point replies in blue and the text added or changed in the revised manuscript in red.

Specific replies

Reply to Reviewer's comments (RC1):

General Comments

The authors provide an informative and insightful analysis of ocean acidification extreme events (OAX) in the North Pacific. They demonstrate the skill of their model in simulating observed OA trends, and they have addressed its representation of mean conditions and variability in a previous study (Desmet et al, 2022). They highlight the regional heterogeneity in frequency and intensity of extreme conditions in a changing climate and point out the processes contributing to regional differences, such as the magnitude of regional variability relative to the long-term trend and the influence of off-shore propagating eddies on property distributions. Additionally, they attribute changing OAX conditions to CO2 increase by comparing to a control simulation based on 1979 conditions. Their analysis of the role of mesoscale eddies in driving regional OAX characteristics is particularly interesting.

Authors: We thank the reviewer for the very supportive comments.

Specific Comments

1) It appears that the model-observation comparisons are made only with surface data. Since an analysis of conditions at depths of up to 250 m is one of the interesting aspects of this study, could the authors provide some evaluation/discussion of model skill at these depths?

Authors: We thank the reviewer for this valuable comment and agree that an evaluation of modeled subsurface OA trends is warranted. However, only a very limited evaluation is possible due to the lack of long-term subsurface observations. The only long-term observations of the marine carbonate system at depth known to us stem from line P based on the work of Franco et al. [2021]. Unfortunately, their analysis is limited to DIC. Still, this is clearly of value. Thus, we added an evaluation of our modeled subsurface DIC trends against these observation-based trends.
The modeled DIC trends (DIC is normalized to a salinity value of 33 psu) are overall well confirmed by the observations, but the model tends to have higher trends than suggested by the observations (Figure 1). Even though there are substantial uncertainties associated with the observation-derived trends, this discrepancy needs to be noted. We discuss the implications of this finding in the caveat section of the revised manuscript. If it holds up to further scrutiny, this model bias would imply a slower increase of the sub-surface OAX than simulated, but no change in our conclusions about the abruptness of the onset of the OAX or the large spatial heterogeneity.

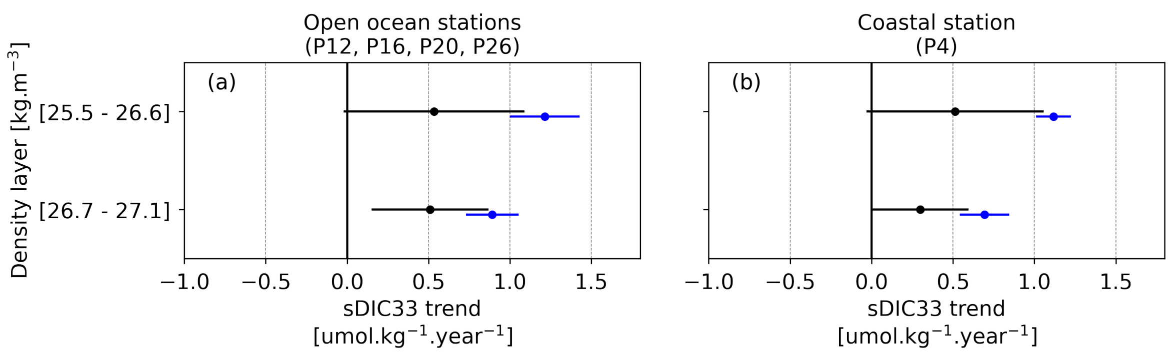

Figure 1: Appendix Figure B2 in revised manuscript: Trends in dissolved inorganic carbon normalized to a salinity value of 33 psu (sDIC33) in the subsurface of line P (in μmol kg^{-1} year^{-1}). (blue) Simulated ROMS-BEC trends and (black) observed trends from Figure 6 in Franco et al. [2021]. The trends have been averaged within two density layers, namely mixed layer/pycnocline waters ([25.5 - 26.6] kg m^{-3}) and intermediate waters ([26.7 - 27.1] kg m^{-3}), as well as across the four open ocean stations (P12, P16, P20, P26) in panel (a). Black error bars denote the average of the two standard deviation credible interval (95% CrI) of individual data points from Figure 6 in Franco et al. [2021], while blue error bars denote the spatial standard deviation across stations and density levels from ROMS-BEC simulated trends.

In response to this comment, we included Figure 1 in the appendix of the revised manuscript. In the revised manuscript, we modified the model evaluation section as follows:

Text added:

Lines 153-161: "While the evaluation of subsurface pH and Ω_A trends is not yet possible given the lack of long-term time series observations, we evaluate the simulated subsurface trends in dissolved inorganic carbon down to about 300 m depth against observations derived from the line P time series [Appendix Figure B2; Franco et al., 2021]. The simulated dissolved inorganic carbon trends (DIC is normalized to a salinity of 33 psu) in the subsurface of line P stations are in the range of observed trends (Appendix Figure B2). However, the model tends to have larger trends than suggested by the observations. In intermediate waters (150-300 m depth), simulated DIC trends are 2% larger than the upper bound of observed trends in open ocean stations, and 15% larger in the coastal station P4 (Appendix Figure B2). We further discuss the implications of this discrepancy in the caveat section

4.4.
Overall, although subsurface trends in dissolved inorganic carbon tend to be overestimated, our model simulates [...]"

We additionally discuss the implications of this evaluation in the caveat section of the revised manuscript as follows:

Lines 494-501: "The use of relative thresholds on fixed baselines to define OAX requires the model to accurately capture OA trends since the ratio of the long-term trend to local variability is key in determining the increase in OAX in that case. Giving us confidence in our results are the well captured pH and Ω_A surface trends over the last four decades by our model. Yet, in the subsurface, simulated dissolved inorganic carbon trends tend to be higher than suggested by observations, even though substantial uncertainties associated with the observation-derived trends exist [Franco et al., 2021]. If this model subsurface bias holds up to further scrutiny and for other carbonate variables such as $[H^+]$, it would imply a slower increase of subsurface OAX than simulated. Yet our conclusions about the large spatial heterogeneity in the progression of OAX and the abruptness of the onset of the OAX in the far offshore regions would remain unchanged."

Besides, as stated in the general comments of the reviewer, we addressed the model representation of the mean conditions of key variables at depth (Figures 2 and 3), as well as the representation of the depth distribution of pH and Ω_A during the North American Carbon Program West Coast Cruise [Feely et al., 2008] (Figure4) in a previous study [Desmet et al., 2022]. The HCast simulation in our manuscript uses the same model configuration and forcing as employed by Desmet et al. [2022]. There were some small changes owing to our use of slightly different initial conditions as a result of a change in the forcing used for the model spin up. While Desmet et al. [2022] used daily fields from the year 1979 as the forcing for the spin up, we use a normal year forcing (apart from atmospheric CO_2, which is transient). The normal year forcing is created by adding daily anomalies of the year 2001 to the climatological mean surface fields of wind stress, short and long-wave radiations, and freshwater fluxes derived from ERA-5 [Hersbach et al., 2020; Copernicus Climate Change Service (C3S), 2017]. The two simulations are therefore not numerically equivalent, but present very similar evaluation results (cf. Figures 2, 3, and 4, and Desmet et al. [2022]).
We address this by adding the following sentences in the methods of the revised manuscript:

Text added:

Lines 115-120: "Our HCast simulation uses slightly different initial conditions than employed by Desmet et al. [2022] as a result of a change in the forcing used for the model spin up. While Desmet et al. [2022] used daily fields from the year 1979 as the forcing for the spin up, we use a normal year forcing (apart from atmospheric CO_2, which is transient). The normal year forcing is created by adding daily anomalies of the year 2001 to the climatological mean surface fields of wind stress, short and long-wave radiations, and freshwater fluxes derived from ERA-5 [Hersbach et al., 2020; Copernicus Climate Change Service (C3S), 2017]."

Lines 138-140: "Although our HCast simulation is not numerically equivalent to the simulation employed by Desmet et al. [2022] owing to the different initial conditions (cf. Section 2.1), they present very similar evaluation results (not shown). Here we further evaluate the surface OA trends in pH and Ω_A of the model against observations (Table 1)."

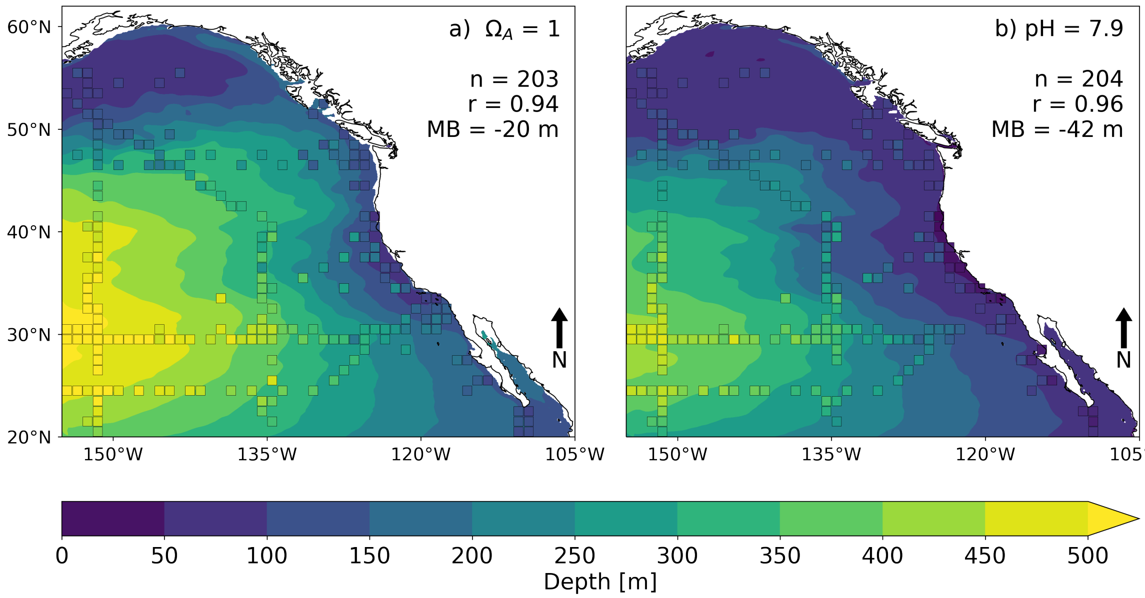

Figure 2: Evaluation of the model (HCast) simulated annual mean depths of (a) the Ω_A saturation horizon (Ω_A=1) and (b) the pH = 7.9 isosurface compared to the corresponding observational estimates based on the 1°×1° gridded GLODAPv2 climatology [Lauvset et al., 2016]. The model simulated results are shown as filled contours, while the (gridded but not mapped) observations are shown as filled squares. Each square stands for the corresponding 1°×1° bin of the gridded product. The corresponding spatial Spearman's correlations (r), spatial mean biases (MB), and number of points (n) used for the calculation are indicated at the top.

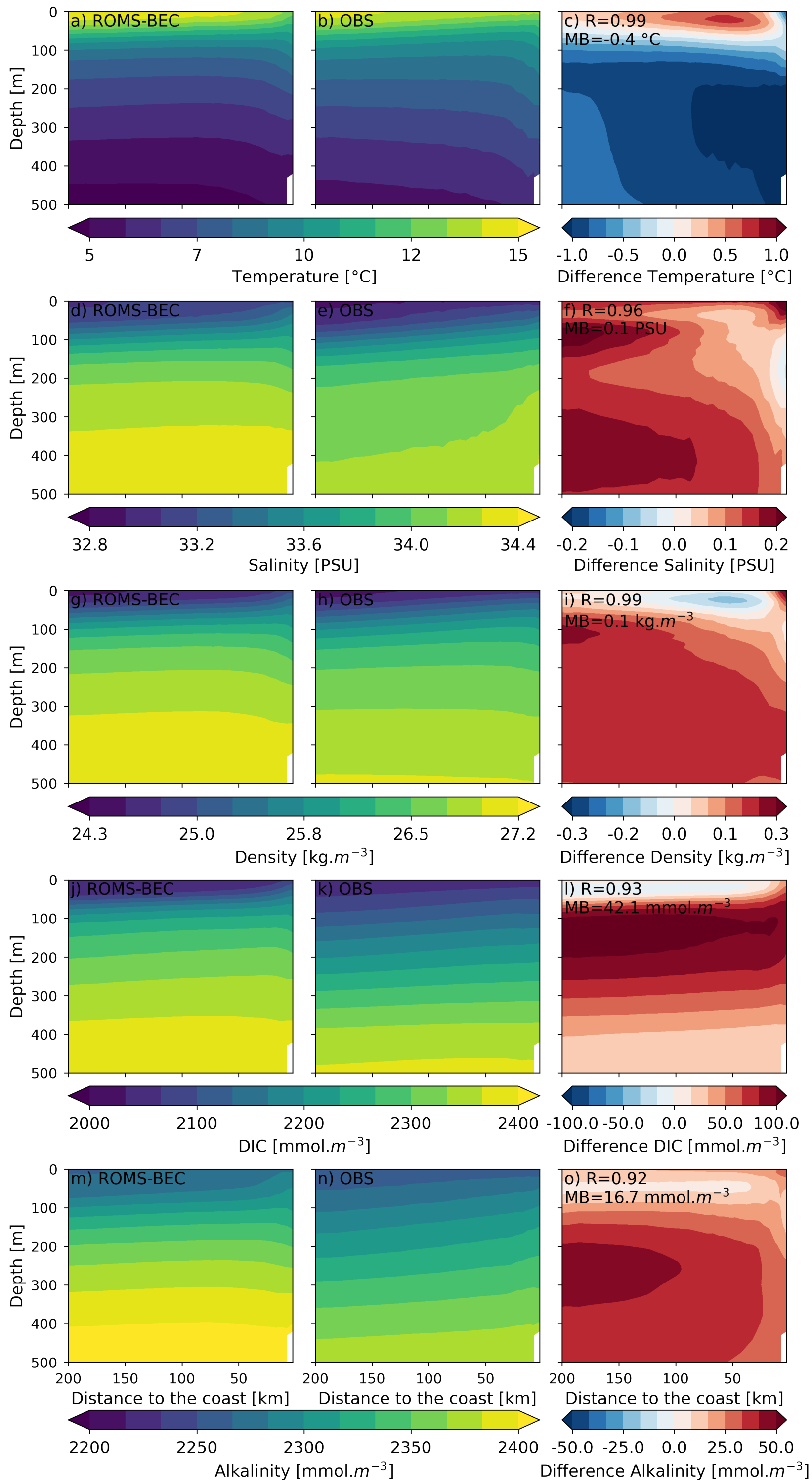

Figure 3: Climatological mean (1984-2019) interior temperature (a-c), salinity (d-f), density (g-i), DIC (j-l) and alkalinity (m-o) in ROMS-BEC (HCast) are evaluated against SODA 1.4.2 [Carton and Giese, 2008] for the temperature, salinity and density, and 1°x1°GLODAPv2 gridded datasets [Lauvset et al., 2016] for DIC and Alkalinity. Spatial correlation (R) and mean bias (MB) are given in each differences plot. Cross-section is averaged over the region denoted by the black contour line in Figure 5a in Desmet et al. [2022] until 200 km from the coast and 500 m depth.

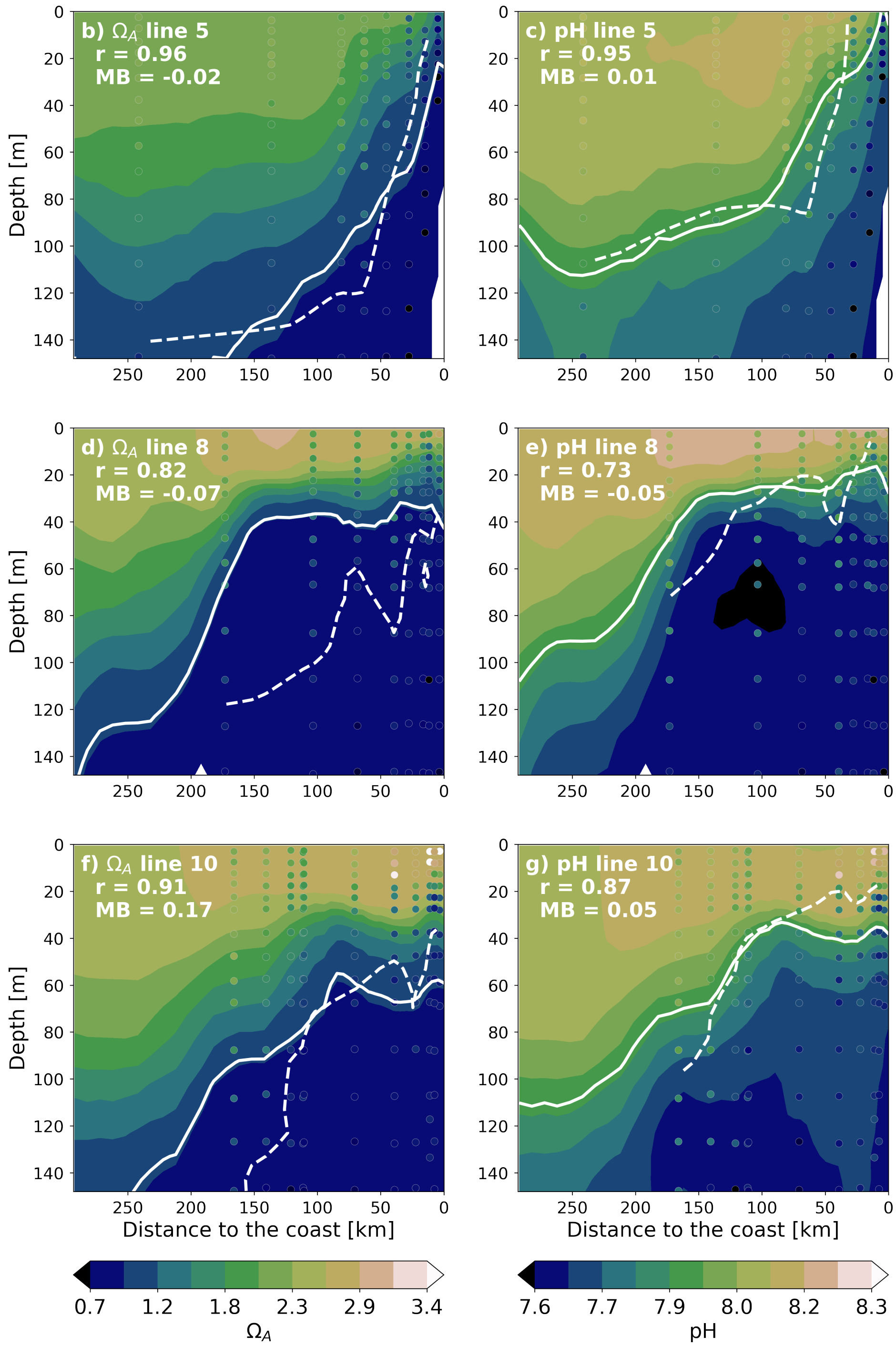

Figure 4: Evaluation of model (HCast) simulated Ω_A and pH against observations from the North American Carbon Program (NACP) West Coast Cruise [Feely et al., 2008]. (a) Map of stations and masks used for simulated fields for each transect, plotted on top of every fifth grid lines of ROMS-BEC grid. (b–g) Offshore transects of (b, d, and f) Ω_A and (c, e, and g) pH at transect 5 (top), 8 (middle), and 10 (bottom) (see map in Figure 2a of Desmet et al. [2022] for locations). The model simulated fields are shown as filled contours, while the observations are shown as filled circles. White lines denote the simulated (solid lines) and observed (dashed) $\Omega_A = 1$ horizon (b, d, and f) and $pH_{7.9}$ isopleth (c, e, and g), respectively. Spearman spatial correlations (r) and mean biases (MB) between model and observations of the interior distribution along those transects are given in the top left corners.

2) Please include some discussion of the altered southern boundary condition in the control run in the context of attribution of OAX events to the rise in atmospheric CO2. How large is the impact of the southern boundary DIC concentration relative to gas exchange within the domain?

Authors: We thank the reviewer for raising this issue. Since the southern lateral boundary of the model is nearly 10 000 km away from the domain used for the analysis, i.e., almost at the antipode of the CCS (Figure 5b), the influence of DIC change at the lateral boundaries on the detected OAX relative to gas exchange is negligible. It is not only the distance, but also the presence of the equator, which forms a strong natural barrier for inter-hemispheric exchange, that prevents signals from the southern boundary to influence our results. Please note that this issue is actually the reason why we opted for such a large domain in the first place, rather than using a regular grid whose domain is smaller, which makes the influence of the lateral boundary conditions much more substantial.

To better reflect the remote position of the southern boundary condition relative to the domain of analysis, we included in Figure 1 of the revised manuscript an additional panel (b) showing the entire telescopic grid and where the position of the southern boundary condition can be seen (Figure 5).

Text added:

Line 110: "[...] except at a few places in the Southern Ocean, i.e., more than 9000 kilometers away from the analysis domain."

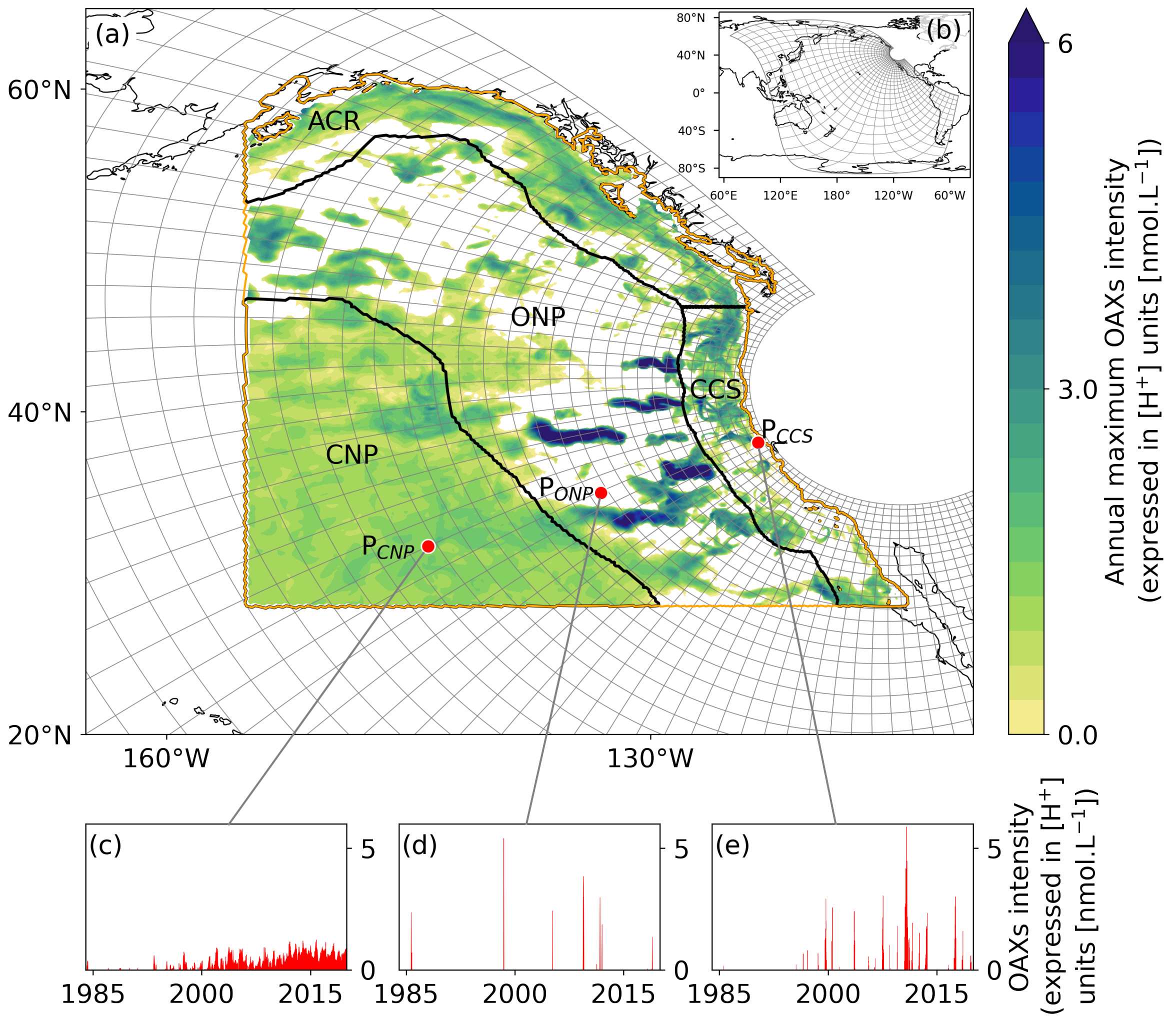

Figure 5: Map of the analysis domain and the selected subregions, and key properties of the diagnosed OAX. (a) Map of the Northeast Pacific with the telescopic grid of the model plotted in grey for every 10^{th} grid cell. The black contours delimit the four selected subregions, i.e., the two coastal regions inshore of 300 km, namely the Alaskan Coastal Region (ACR) and the California Current System (CCS), and the two open ocean regions, i.e., the Offshore Northeast Pacific (ONP) and the Central Northeast Pacific (CNP). The domain of analysis is denoted by the orange contour line. The annual maximum intensity of the simulated OAXs in year 2014 at 100 m depth is plotted on top. White regions indicate that no OAX occurred in that year at this depth. (b) Map of the whole ROMS-BEC telescopic grid, plotted for every 20^{th} grid cell. (c-e) Time series of $[H^+]$ intensity at 100 m depth at the three locations depicted by red points in (a), i.e., (left) P_{CNP} in the CNP region (31.66°N-143.77°W), (middle) P_{ONP} in the ONP region (34.97°N-133.07°W), and (right) P_{CCS} in the CCS (38.08°N-123.32°W).

Is the removed trend in DIC fully attributable to atmospheric CO2 increase or could there be a contribution associated with interannual variability?

Authors: We thank the reviewer for this relevant question. First of all, we would like to refer to the answer to the previous comment in that the exact nature of these Southern Ocean boundary conditions have a negligible impact on our study region. We still paid attention to these boundary condition, since we are using this simulation also for studies elsewhere in the Pacific. Thus onward to the specific question raised by the reviewer: Yes, the removed trend in the Southern Ocean DIC boundary condition is fully attributable to atmospheric CO_2 since the transient DIC boundary condition was created by using the GLODAPv2 climatological preindustrial DIC and time evolving anthropogenic carbon fields (transient steady-state approach and the anthropogenic CO_2 fields of Sabine et al. (2004) as described in Desmet et al. 2022). There is no contribution associated with interannual variability since there is no interannual variability in the first place. However, since the anthropogenic contribution is not fully linear there is a slight modulation once the linear trend is removed for the Cons simulation (Figure 6).

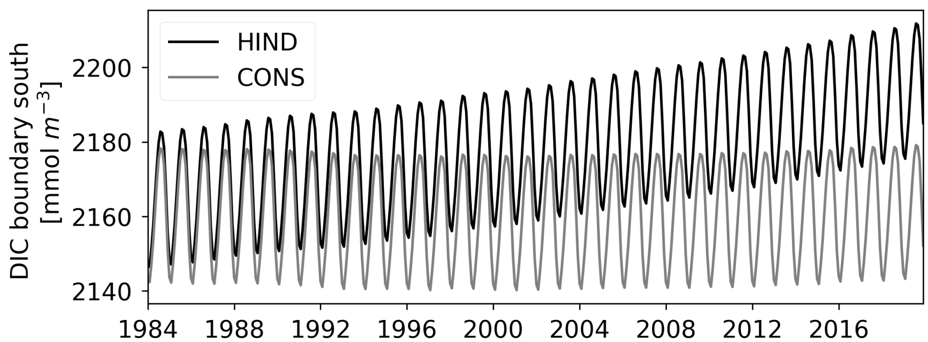

Figure 6: DIC concentration (in mmol m^{-3}) at the southern boundary condition in the case of the HCast (black, HIND) and CCons (grey,CONS) simulations.

In the methods of the revised manuscript, we increased clarity with regard to the absence of interannual variability in the transient DIC concentration of the southern boundary as follows:

Line 112: "The first one corresponds to the simulation used by Desmet et al. [2022] and consists of a hindcast simulation (HCast) from 1979 through 2019, where atmospheric pCO_2 is prescribed to increase according to observations [Landschützer et al., 2020], and where the DIC concentration at the lateral southern open boundary of the model is transient, but does not include interannual variability."

3) In the context of relative threshold, fixed baseline stressor detection, the authors highlight the importance of the ratio of the long-term trend to local variability in determining OAX increase. Could they also shed light on whether temporal changes in the variability contribute? For instance, does the magnitude of variability increase in some regions? This is addressed to an extent by Figure B4, but I find the histograms difficult to interpret due to their small size.

Authors: We thank the reviewer for those interesting questions and comments. From 1984 to 2019, the magnitude of the variability of [H^+] (annual standard deviation) increases in all surface regions and in the subsurface of the CCS, ONP and CNP regions in the HCast simulation (Figure 7). We agree with the reviewer that it would be interesting to shed light on the contribution of those temporal changes in [H^+] variability to the increase in OAX. However, some of those changes in [H^+] variability also occur in the CCons simulation, e.g., the increase in the ONP 100-250 m depth layer (Figure 7). The simulated changes in variability are therefore not only driven by the increase in atmospheric CO_2, but can also be driven by decadal climate modes or climate change feedback such as changes in temperature, etc. Based on the two available simulations, it is therefore not trivial to thoroughly attribute the contribution of the trend in [H^+] versus the variability change to OAX increase.
Yet, we estimated for regions with Gaussian [H^+] distributions (e.g., at 100 m depth of P_{CCS}), i.e., under the assumption of a Gaussian distribution, that the change in variability would only lead to a 1.3 fold increase in OAX days versus a 14-fold increase from the change in mean state (long-term trend). Similarly, it would only lead to a 2% increase in the maximum OAXs intensity versus a 82% increase from the change in mean state.

In order to shed light on whether temporal changes in the variability occur and whether they contribute to OAX increase, we added Figure 7 below to the appendix of the revised manuscript. In the discussion of the revised manuscript, we further discuss those questions in a newly added paragraph as follows:

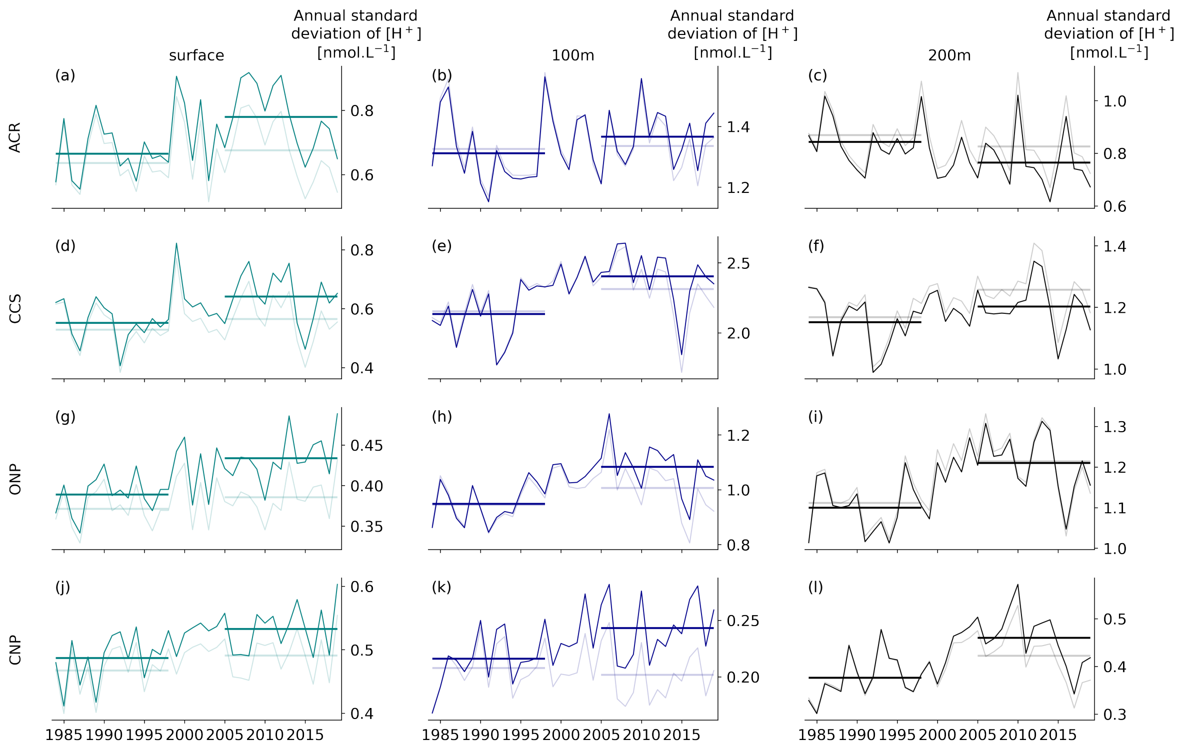

Figure 7: Changes in annual standard deviation of $[H^+]$ in the HCast (dark) and CCons (light) simulations for the four regions (rows) and three depth layers (columns). The horizontal lines depict the average standard deviation during the 15 first and last years of the analysis period for each simulation.

Text added:

Lines 388-398: "When using a relative threshold and a fixed baseline to define OAX, the ratio of the long-term trend to local variability is key in determining the increase in OAX. Thus temporal changes in the variability can have a substantial influence on the evolution of the OAX. Such an increase in variability is actually expected as a consequence of ocean acidification [see also Burger et al., 2020], driven by the increase in the hydrogen ion concentration and a higher sensitivity to change. The variability can also change as a consequence of changes in weather and climate. In our simulations, the variability of $[H^+]$ increases in all surface regions and in the subsurface of the CCS, ONP, and CNP regions (Appendix Figure B5). However, these increases in variability tend to contribute comparatively little to the overall increases in the OAX. We can estimate this contribution most easily in the regions where the $[H^+]$ distributions are Gaussian (e.g., at 100 m depth of P_{CCS}). There, the increase in variability increases the number of OAX days by a factor of 1.3, which is an order of magnitude smaller than the impact of the change in the mean state, as this leads to a 14-fold increase. Similarly, the maximum OAX intensity would increase by only 2% from the change in variability, versus the intensity increases by 82% from the change in mean state.

Technical corrections

Line 49: please add citation. We thank the reviewer for pointing out that a citation was missing and added the corresponding citation in the revised manuscript (Burger et al., 2020)

Figure 1: Please consider rephrasing "[H+] intensity" to reflect that it is the intensity of high [H+] events. Perhaps something like "[H+] event intensity"
We thank the reviewer for this valuable comment for enhancing the clarity of the manuscript and modified the caption of Figure 1 in the revised manuscript as follows: "OAXs intensity (expressed in

[H+] units [nmol.L-1])"

Line 231: "this horizon shoals by 50 m on average". Is this the average over the whole domain or the coastal areas?
We thank the reviewer for asking the question and pointing out that the message was not clear in the manuscript. It is the average over coastal areas only, and it shoals by 45 m to be more precise. In response to the reviewer question, we increased both precision and clarity by modifying the revised manuscript as follows: Line 246: "[...] shoals by 45 m on average in coastal areas, [...]"

Line 532: Are the units on sigma degrees latitude? We thank the reviewer for the question. Sigma is the standard deviation for Gaussian kernel for the smoothing so units are indeed degrees latitude. We added the units in the revised manuscript.

References

Burger, F. A., J. G. John, and T. L. Frölicher, 2020: Increase in ocean acidity variability and extremes under increasing atmospheric CO2. *Biogeosciences*, 4633–4662, doi:https://doi.org/10.5194/bg-17-4633-2020.

Carton, J. A. and B. S. Giese, 2008: A reanalysis of ocean climate using Simple Ocean Data Assimilation (SODA). *Monthly Weather Review*, **136**, 2999–3017, doi:https://doi.org/10.1175/2007MWR1978.1.

Copernicus Climate Change Service (C3S), 2017: ERA5: Fifth generation of ECMWF atmospheric reanalyses of the global climate. *Copernicus Climate Change Service Climate Data Store (CDS),29/08/2020*.

Desmet, F., N. Gruber, E. E. Köhn, M. Münnich, and M. Vogt, 2022: Tracking the space-time evolution of ocean acidification extremes in the California Current System and Northeast Pacific. *Journal of Geophysical Research: Oceans*, 1–30, doi:10.1029/2021jc018159.

Feely, R. A., C. L. Sabine, J. M. Hernandez-Ayon, D. Ianson, and B. Hales, 2008: Evidence for upwelling of corrosive "acidified" water onto the continental shelf. *Science*, **320**, 1490–2, doi:https://doi.org/10.1126/science.1155676.

Franco, A. C., D. Ianson, T. Ross, R. C. Hamme, A. H. Monahan, J. R. Christian, M. Davelaar, W. K. Johnson, L. A. Miller, M. Robert, and P. D. Tortell, 2021: Anthropogenic and Climatic Contributions to Observed Carbon System Trends in the Northeast Pacific. *Global Biogeochemical Cycles*, **35**, 1–21, doi:10.1029/2020GB006829.

Hersbach, H., B. Bell, P. Berrisford, S. Hirahara, A. Horányi, J. Muñoz-Sabater, J. Nicolas, C. Peubey, R. Radu, D. Schepers, A. Simmons, C. Soci, S. Abdalla, X. Abellan, G. Balsamo, P. Bechtold, G. Biavati, J. Bidlot, M. Bonavita, G. De Chiara, P. Dahlgren, D. Dee, M. Diamantakis, R. Dragani, J. Flemming, R. Forbes, M. Fuentes, A. Geer, L. Haimberger, S. Healy, R. J. Hogan, E. Hólm, M. Janisková, S. Keeley, P. Laloyaux, P. Lopez, C. Lupu, G. Radnoti, P. de Rosnay, I. Rozum, F. Vamborg, S. Villaume, and J. N. Thépaut, 2020: The ERA5 global reanalysis. *Quarterly Journal of the Royal Meteorological Society*, **146**, 1999–2049, doi:https://doi.org/10.1002/qj.3803.

Landschützer, P., G. G. Laruelle, A. Roobaert, and P. Regnier, 2020: A uniform pCO2 climatology combining open and coastal oceans. *Earth System Science Data*, **12**, 2537–2553, doi:https://doi.org/10.5194/essd-12-2537-2020.

Lauvset, S. K., R. M. Key, A. Olsen, S. Van Heuven, A. Velo, X. Lin, C. Schirnick, A. Kozyr, T. Tanhua, M. Hoppema, S. Jutterström, R. Steinfeldt, E. Jeansson, M. Ishii, F. F. Perez, T. Suzuki, and S. Watelet, 2016: A new global interior ocean mapped climatology: The 1° × 1° GLODAP version 2. *Earth System Science Data*, doi:https://doi.org/10.5194/essd-8-325-2016, iSBN: 1866-3591.